

Photonic immobilization techniques used for the detection of cardiovascular disease biomarkers

Goncalves, Odete; Banuls, Maria-Jose; Alonso, Rafael; Jimenez-Meneses, Pilar; Maquieira, Angel; Vorum, Henrik; Petersen, Steffen B.; Neves-Petersen, Maria Teresa

Published in:
Biophotonics

DOI (link to publication from Publisher):
[10.1117/12.2305717](https://doi.org/10.1117/12.2305717)

Publication date:
2018

Document Version
Publisher's PDF, also known as Version of record

[Link to publication from Aalborg University](#)

Citation for published version (APA):

Goncalves, O., Banuls, M.-J., Alonso, R., Jimenez-Meneses, P., Maquieira, A., Vorum, H., Petersen, S. B., & Neves-Petersen, M. T. (2018). Photonic immobilization techniques used for the detection of cardiovascular disease biomarkers. In J. Popp, VV. Tuchin, & FS. Pavone (Eds.), *Biophotonics: Photonic Solutions for Better Health Care VI* (Vol. 10685). Article 106852Z-1 SPIE - International Society for Optical Engineering. <https://doi.org/10.1117/12.2305717>

General rights

Copyright and moral rights for the publications made accessible in the public portal are retained by the authors and/or other copyright owners and it is a condition of accessing publications that users recognise and abide by the legal requirements associated with these rights.

- Users may download and print one copy of any publication from the public portal for the purpose of private study or research.
- You may not further distribute the material or use it for any profit-making activity or commercial gain
- You may freely distribute the URL identifying the publication in the public portal -

Take down policy

If you believe that this document breaches copyright please contact us at vbn@aub.aau.dk providing details, and we will remove access to the work immediately and investigate your claim.

PROCEEDINGS OF SPIE

SPIDigitalLibrary.org/conference-proceedings-of-spie

Photonic immobilization techniques used for the detection of cardiovascular disease biomarkers

Odete Gonçalves, María-José Bañuls, Rafael Alonso, Pilar Jiménez-Meneses, Ángel Maquieira, et al.

Odete Gonçalves, María-José Bañuls, Rafael Alonso, Pilar Jiménez-Meneses, Ángel Maquieira, Henrik Vorum, Steffen B. Petersen, Maria Teresa Neves-Petersen, "Photonic immobilization techniques used for the detection of cardiovascular disease biomarkers," Proc. SPIE 10685, Biophotonics: Photonic Solutions for Better Health Care VI, 106852Z (17 May 2018); doi: 10.1117/12.2305717

SPIE.

Event: SPIE Photonics Europe, 2018, Strasbourg, France

Photonic immobilization techniques used for the detection of cardiovascular disease biomarkers

Odete Gonçalves^a, María-José Bañuls^b, Rafael Alonso^b, Pilar Jiménez-Meneses^b, Ángel Maquieira^b, Henrik Vorum^c, Steffen B. Petersen^a and Maria Teresa Neves-Petersen^{*a,c}

^a Department of Health Science and Technology, Aalborg University, Fredrik Bajers vej 7, DK-9220, Aalborg, Denmark

^b Instituto Interuniversitario de Investigación de Reconocimiento Molecular y Desarrollo Tecnológico (IDM) Universitat Politècnica de València, Universitat de València, Spain.

^c Department of Clinical Medicine, Aalborg University, Denmark

ABSTRACT

In today's point-of-care testing (POCT), there is an ever-increasing demand for novel and more efficient devices for early diagnosis, especially in cardiovascular diseases (CVD). Early detection of CVD markers, such as Troponin present in the bloodstream, is a key factor for reducing CVD mortality rates.

Thiol-ene coupling (TEC) and Light Assisted Molecular Immobilization (LAMI) are photonic techniques leading to immobilization of bioreceptors, such as, antibodies which recognize cardiac markers. These techniques present advantages compared to traditional immobilization techniques since, e.g., there are no thermal or chemical steps and they work in water media. TEC reaction takes place at close-to-visible wavelengths ($\lambda=365\text{nm}$) which induces the formation of thiol radicals which bind to alkene functional group on the surface through a thioether bond. LAMI secures molecular immobilizations in a spatially oriented, localized and covalent coupling of biomolecules onto thiol reactive surfaces down to submicrometer spatial resolution. LAMI is possible due to a conserved structural motif in proteins: the spatial proximity between aromatic residues and disulfide bridges. When aromatic residues are excited with UV light (275-295nm), disulphide bridges are disrupted and free thiol groups are formed that can bind covalently to a surface decorated with thiol groups.

We have achieved successful immobilization of anti-troponin and anti-myoglobin antibodies with both photonic immobilization techniques. The microarrays of immobilized monoclonal antibodies have successfully detected the CVD biomarkers troponin I and myoglobin, as confirmed by fluorescence imaging. A sandwich immunoassay was carried out, Troponin I and Myoglobin were detected down to 10 ng/mL and 1 ng/mL, respectively.

Keywords: Point-of-care testing (POCT), cardiovascular diseases (CVD), Light Assisted Molecular Immobilization (LAMI), Thiol-ene coupling (TEC), Troponin, Myoglobin, UV light.

1. INTRODUCTION

Cardiovascular diseases (CVD) are a leading cause of mortality worldwide. According to the World Health Organization (WHO), 31% of global deaths (estimated 17.7 million people) in 2015 were due to CVD¹. Early and accurate diagnosis and timely treatment is therefore crucial for the reduction of CVD related mortality. Cardiac biomarkers are essential tools for an early and prompt diagnosis and effective treatment. Over the years, many researchers have lead great effort in the identification of such biomarkers. Investigation on different kinds of biomarkers for different aspects of CVD remains an important research field. With different applications and uses, from screening and prognosis to diagnosis, many biomarker have been studied and identified and many are under evaluation^{2,3}. In this paper, we will focus on two specific biomarkers, usually used for diagnostic purposes on Myocardial Injury: Myoglobin and Troponin I.

*nevespetersen@gmail.com Phone: +45 22522475

Myoglobin is already established as a cardiac disease biomarker, although it is only used together with other cardiac biomarkers such as Troponin and Creatine kinase-MB (CK-MB). Although it is not specific to cardiac muscle tissue (it can also be found in skeletal muscle tissue), it is the first protein to be released upon damage of myocardial muscle cells⁴.

Cardiac Troponin (cTn) has been the biomarker of choice for early detection of cardiac injury due to its specificity and to the prolonged time elevated troponin values can be found in circulation⁵. Troponin is composed of three subunits: cTnC, cTnI and cTnT. It plays a major role in the control of cardiac muscle contraction and relaxation controlled by Ca^{2+} regulation. cTnC is responsible for the reception of Ca^{2+} , while cTnI and cTnT make a transduction of this Ca^{2+} binding signal and are involved in multiple interactions with actin and troponomyosin (to which cTnT is the binding subunit of the cTn complex^{6,7}. All these subunits present tissue-specific isoforms. cTnC is not commonly used as a CVD biomarker due to the unspecificity of its cardiac isoform (which is shared by slow-twitch skeletal muscles)⁸. cTnI and cTnT provide comparable information, although some exceptions have been reported⁵.

Point of care testing (POCT) has been increasing in recent years as a growing awareness of the importance of patient centered treatment and importance of fast and portable ways to reach an analytical result. Cardiac POCT in particular, have been the focus of many researchers in an effort to improve the performance of the already existing POCT^{9,10}.

Biosensors are a crucial part of these POCT devices and their immobilization to a sensing surface an important step in biosensor production. There are many factors involved in this process that influence biosensor performance, such as the support nature, chemistry of attachment, biosensor orientation and density and reproducibility. Many techniques were developed to achieve biosensor attachment such as, adsorption, electrostatic interactions and covalent binding. One of the preferred methods for biosensor attachment to a sensing surface is covalent binding, as it allows for an oriented and controlled binding and also provides strong and stable binding of the biosensors¹¹. In the present study, two photonic immobilization techniques are presented: Thiol-ene coupling (TEC) and Light Assisted Molecular Immobilization (LAMI). Both techniques were applied in the immobilization of anti-myoglobin and anti-cTnI antibodies for the detection of both cardiac biomarkers.

TEC chemistry meets the main characteristics of the highly interesting click-chemistry reactions¹² including: high yields, region specificity, mild reaction conditions, and tolerance to a variety of functional groups^{12–14}. It consists of the covalent coupling between an alkene group on the surface and free thiol moieties on the probe. TEC reactions take place at close-to-visible wavelengths ($\lambda=365\text{ nm}$) which induces the thiol radical formation that links to alkene functional group by means of a thioether bond (Figure 1). The approach is fast, clean, and permits to perform localized attachment of biomolecules. Moreover, this procedure is compatible with aqueous media chemistry, which is critical for its bioavailability.

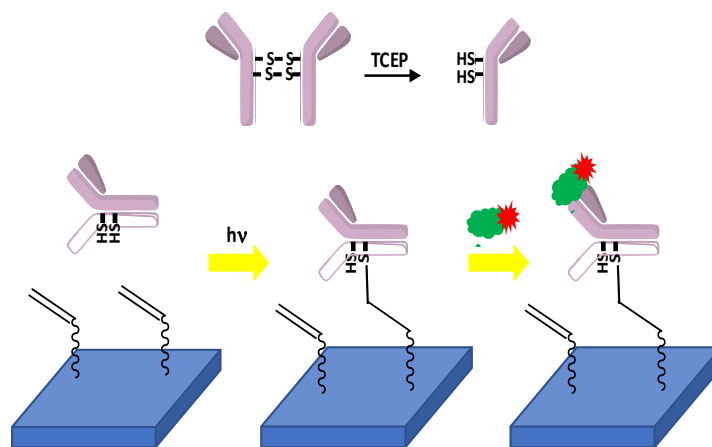


Figure 1. Schematic representation of Thiol-ene coupling (TEC). Tris(2-carboxyethyl)phosphine (TCEP).

This reaction has been previously employed to construct competitive DNA microarrays without the need of blocking the support surface^{15–17}. The cysteine residues in antibodies are mostly oxidized, forming disulphide bridges, and it is

necessary to create free thiol moieties to perform TEC attachment. For this purpose, the hinge-region disulfide bonds of the whole antibody are selectively reduced. After this cleavage step, the two resulting half-antibodies can be immobilized onto the surface employing TEC, without hindering or adversely affecting antigen-binding function.

LAMI resorts to UV light (280-295 nm), exciting the aromatic residues (Tryptophan, Tyrosine and Phenylalanine) present in the protein, which leads to the breakage of nearby disulphide bridges and formation of free thiol groups^{18,19}. These newly formed thiol groups will then be able to bind in a spatially oriented and covalent manner to free thiol groups present in the support surface¹⁹ (Figure 2). This technique is based on a conserved motive in proteins, where spatial proximity of aromatic residues to disulphide bridges is observed. One such conserved motif is present at the bottom of the Fab fragments in immunoglobulins²⁰. Aromatic residues such as Tryptophan and Tyrosine are the best absorbers at 280nm^{21-24,24,25}.

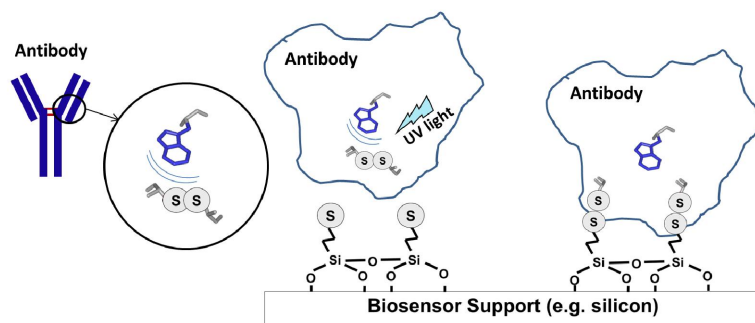
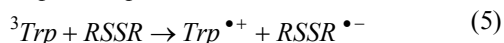
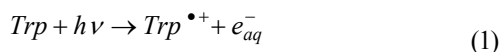


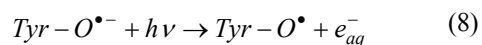
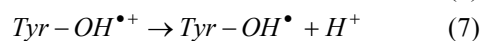
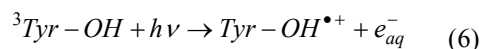
Figure 2. Schematic representation of Light Assisted Molecular Immobilization (LAMI).

UV light excitation of the side chains of these aromatic residues can lead to a cascade of photochemical processes upon their excitation to a higher energy state followed by subsequent relaxation to the ground state²⁶⁻²⁸. One such process is photoionization, where an electron is ejected to the aqueous medium and becomes caged by water molecules, leading to the formation of a solvated electron (e_{aq}^-)²⁹ (scheme 1). This solvated electron may lead to the formation of a disulphide electron adduct when reacting with a nearby disulphide bridge (schemes 5 and 9), which ultimately dissociates and breaks the disulphide bridge, forming free thiol groups (schemes 11 and 12).

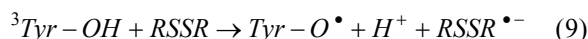
Formation of solvated electrons upon excitation of Trp may result from a non-radiative relaxation after excitation, yielding a neutral radical Trp^{\bullet} derived from $Trp^{\bullet+}$ radical cation (schemes 1 and 2). A disulfide bridge electron adduct $RSSR^{\bullet-}$ may also be formed due to electron transfer from the triplet state 3Trp , yielded from intersystem crossing of excited Trp (schemes 3-5).



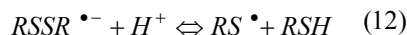
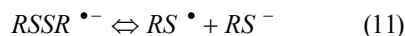
Tyrosine may also undergo diverse photochemical processes such as the ones displayed in schemes 6 to 8 (formation of radical cation $Tyr-OH^{\bullet+}$, neutral radicals $Tyr-OH^{\bullet}$ and $Tyr-O^{\bullet}$ and solvated electron (e_{aq}^-)).



The triplet state of Tyr can promptly be quenched by a nearby disulphide bridge or Trp (scheme 9)



UV excitation of aromatic residues such as Tyr and/or Trp may lead to the formation of solvated electrons, as previously shown. The solvated electrons may, in turn, be captured by cystines and result in the breakage of the SS bridge (scheme 10-12)



The reduction of SS bridges upon UV light excitation of the aromatic residues has been demonstrated in various types of proteins such as cutinase^{18,19}, bovine serum albumin²³, prostate specific antigen²¹, insulin³⁰, plasminogen³¹, C-Reactive protein³², alpha-lactalbumin³³, lysozyme³⁴, and antibody Fab fragments²¹. Moreover, immobilization with submicrometer spatial resolution through LAMI has also been reported previously^{22,24}.

Light Assisted Molecular Immobilization (LAMI) and Thiol-ene coupling (TEC) are two photonic techniques that allow for biosensor immobilization in a covalent manner, with the advantage of surpassing any need for chemical or thermal steps to achieve molecular attachment of the biosensors to the support. Successful immobilization of cTnI and anti-myoglobin antibodies with both photonic immobilization techniques was achieved and the immobilized monoclonal antibodies have successfully detected the CVD biomarkers cTnI and myoglobin, as confirmed by fluorescence imaging. Immunoassays were carried out and cTnI and myoglobin were detected down to 10 ng/mL and 1 ng/mL, respectively.

2. MATERIAL AND METHODS

2.1. Protein and Buffer Solutions

Monoclonal mouse anti-cardiac troponin I (cTnI) 19C7cc was purchased from HiTest (Turku, Finland). Natural Cardiac Troponin I protein was purchased from Abcam (Cambridge, UK). Troponin I Type 3 (cardiac) monoclonal Antibody (16A11) [Alexa Fluor® 647] was purchased from Novus Biologicals. Primary monoclonal Anti-Myoglobin antibody [BDI927], Natural Human Myoglobin protein, secondary polyclonal Anti-Myoglobin antibody and DyLight® 488 Fast Conjugation Kit for secondary Anti-Myoglobin antibody labelling were purchased from Abcam. Human serum and Bovine Serum Albumin, used in the assay buffer, and NaCl, KCl, Na₂HPO₄•7H₂O and KH₂PO₄ used to prepare PBS buffer were purchased from Sigma Aldrich (Steinheim, Germany).

2.2 TEC

2.2.1 Surface chemistry

Slides were cut into pieces of $\approx 2 \times 1$ cm², cleaned with water and 2-propanol, and then air-dried. Afterwards they were placed in the UV-ozone cleaner (FHR UVOH cleaner, Germany) and irradiated for 10 min at 254 nm. Subsequently, chips were immersed in a solution of triethoxyvinylsilane 2% in toluene for 2 h at room temperature. Finally, chips were washed with 2-propanol and air-dried before being baked for 20 min at 100°C. The surface was characterized by the WCA (water contact angle), with evidence for the presence of alkene groups on the surface shown in all cases.

2.2.2 Illumination setup

In the case of irradiation at 254 nm, the illumination set up consisted of a UV light irradiation lamp ($\lambda = 254$ nm –FHR, UV-ozone technology UVOH, 50 mW/cm²) irradiating for several seconds. In the case of irradiation at 365 nm, the printed functionalized surface was exposed to UV-light at 365 nm with a mercury capillary lamp (6 mW/cm², Jelight Irvine, CA, USA) placed at a fixed distance (≈ 0.5 cm) from the slide for 20 min to induce the immobilization.

2.2.3 Photonic immobilization of primary monoclonal antibodies

Initially, the antibodies were subjected to cleavage into two halves by selective chemical reduction. For that IgG in acetate buffer was incubated with 25 mM tris(2-carboxyethyl)phosphine (TCEP) at 37°C. The corresponding half-IgG were purified by employing a 50 kDa centrifugal filter unit. The concentrations of the solutions were determined by a NanoDrop spectrophotometer.

Microarrays were printed over the previously functionalized glass chips employing a low volume non-contact dispensing system from Biodot (Irvine, CA, USA, model AD1500). 5 minutes after printing the chips were submitted to UV light irradiation ($\lambda = 254$ nm –FHR, UV-ozone technology UVOH. Afterwards, the chips were stored in the dark for 10 min and then, washed with PBS-T for 15 min with stirring, then rinsed with water and dried.

2.2.4 Immunoassays

Firstly, the Myoglobin and the detection anti-cTnI antibody were labelled with a tag. For that, 1 mg of protein was dissolved in 0.1 mL of bicarbonate buffer. Amine-reactive Alexa Fluor 647 (0.1 mg) was dissolved in 0.01 mL of DMSO and the resulting solution was immediately added to the solution of protein while stirring. The resulting mixture was protected from ambient light and stirred at room temperature for 1 h. The reaction mixture was purified by employing 30 kDa centrifugal filter units. The concentration and the label to probe ratio were determined by spectrophotometry.

For the direct immunoassay to detect Myoglobin, the microarrays having immobilised hIgG anti-Myoglobin antibodies were incubated with decreasing concentrations of labelled protein (100, 50, 10, 5 and 1 ng/mL) diluted in PBS-T, for 30 min at room temperature. Afterwards, they were washed with PBS-T and water, and dried.

For the sandwich immunoassay for cTnI, after creating the microarray, the chip was incubated with decreasing concentrations of cTnI (5, 2, 1, 0.5, 0.2, 0.1 and 0.05 $\mu\text{g/mL}$) diluted in PBS containing 10% of human serum for 30 min at room temperature. Then, the chips were washed with PBS-T and water, and dried. Finally, they were incubated with labeled anti-cTnI antibody at 5 $\mu\text{g/mL}$ in PBS-T, for 30 min at room temperature, washed with PBS-T and water, and dried.

2.2.5 Array imaging

The fluorescence of the dried chips was measured employing a homemade surface fluorescence reader equipped with a high sensitive charge couple device camera Retiga EXi from Qimaging Inc, (Burnaby, Canada) and light emitting diodes Toshiba TLOH157P as the fluorescence excitation light source (SFR). Alternatively, the chips were read with a microarray scanner, a GenePix 4000B Microarray Scanner (Axon instruments). Microarray image treatment and quantification were done using the GenePix Pro 4.0 software from Molecular Devices, Inc. (Sunnyvale, CA, USA).

2.3. LAMI

2.3.1 SOi (Silicon on insulator) surface chemistry

Planar SOi surfaces were kindly provided by Centro de Tecnología Nanofotónica de Valencia-Universidad Politécnica de Valencia (NTC-UPV). The surfaces were first hydroxylated in a solution of $\text{K}_2\text{S}_2\text{O}_8$ (200 ml ionized/destilled water + 10.0g $\text{K}_2\text{S}_2\text{O}_8$) at $\approx 99^\circ\text{C}$ for 60 min and afterwards cleaned with pure water and dried using compressed air. After hydroxylation, silanization was performed with a thiol based silane. The surfaces were submerged in a solution of 0.3% v/v 3-mercaptopropyl-trimethoxysilane in m-xylene for 30 min. Subsequently, the surfaces were washed with pure xylene, 70% ethanol and deionized water, dried with compressed dry air and placed in an oven at 100°C for 60 min.

2.3.2 One-photon UV optical setup

The optical experimental setup used for the illumination and immobilization of the biosensors onto the thiol derivatized SOi planar surfaces and the software used to control the experimental setup were described elsewhere³².

Briefly, the Tsunami XP (Spectra-Physics) femtosecond laser source (100fs pulse width and 80MHz repetition rate) was pumped by the Millennia eV (Spectra-Physics). The Tsunami laser source is manually tunable in a range between 700-1080nm. For LAMI illumination, the laser is commonly tuned to 840nm. The 840nm beam output is directed to a harmonic generation module and its frequency tripled to obtain ≈ 280 nm. The third harmonic is then directed into the illumination setup through a different path of the fundamental 840nm beam. The third harmonic beam at 280nm passes through a computer controlled attenuator (PR50CC, Newport) and a polarized beam cube. Power is monitored by a

photodiode placed after each attenuator. In order to control sample exposure to light, the beam is also directed through safety shutters (LS6S2ZM1, VINCENT ASSOCIATES) which are coordinated with the software that controls the microfabrication stage. A CCD camera (MCE-B013-UW, MIGHTEX) is placed above the objective through which the 280nm light is ultimately directed onto the sample, allowing for sample visualization.

No attempts were made to exclude oxygen from the samples studied.

2.3.3 Secondary antibody anti-myoglobin labelling

The secondary anti-myoglobin antibody was labeled with DyLight® 488 Fast Conjugation Kit according to the manufacturer's instructions. Briefly, 10 μL of DyLight® 488 Modifier reagent were added to 100 μL of secondary anti-myoglobin antibody. This mix was then added to lyophilized DyLight® 488 Conjugation Mix and resuspended using a pipette. The conjugation reaction was performed in the dark, at room temperature for 1h. After 1h incubation, 10 μL of DyLight® 488 Quencher reagent were added to the mix and resuspended gently with a pipette. No purification step was required, as indicated in the kit's instructions.

2.3.4 Photonic immobilization of primary monoclonal antibodies

Each primary monoclonal antibody, anti-cTnI and anti-Myoglobulin, was freshly diluted to a concentration of 10 μM in PBS 1x. A droplet of 1 μL of each solution was placed on the thiol derivatized SO_i surface and allowed to dry at room temperature. Subsequently, the samples were placed in the sample holder of the optical illumination setup and the UV light focused onto the surface by manually adjusting the focal distance of the objective (40x) through which the UV light is directed. The samples were then illuminated with 60 μW (power output from the objective) 280nm light, at a velocity of 100 $\mu\text{m/s}$, according to a line pattern (20 lines, 25 μm apart, 1500 μm length) previously uploaded to the command software of the moving stage. After illumination, the samples were washed overnight in a 0.1% PBST (PBS 1x + 0.1% Tween 20) solution. Afterwards, they were cleaned with PBS 1x and dried using compressed air.

2.3.5. Sandwich Immunoassay

In Figure 3 is depicted the general protocol for the sandwich immunoassay after primary antibody immobilization. The target proteins were diluted in assay buffer (PBS + BSA 0.1% + Tween 0.1% + EDTA 5mM + 1% Human Serum) to the final concentrations of 4 μM and 4 nM (cTnI) and 3 nM (Myoglobin). 2 μL of cTnI and Myoglobin were then added to the respective immobilized monoclonal antibodies and incubated for 2h at room temperature on a wet chamber. After incubation, the surfaces were rinsed with PBST 0.1% followed by PBS 1x and dried using compressed air. Subsequently the fluorescently labelled secondary anti-cTnI antibody and secondary anti-Myoglobin antibody were added at a concentration of 0.5 μM in assay buffer and incubated for 1.5h at room temperature on a wet chamber. After incubation the surface was once again washed with PBST 0.1% followed by PBS 1x and dried using compressed air.

3. RESULTS AND DISCUSSION

3.1 Monoclonal Anti-Myoglobin immobilization with TEC and Immunorecognition

hIgG anti-Myoglobin antibodies were immobilised onto alkene functionalized surfaces creating microarrays of 4x2 spots, at 50 $\mu\text{g/mL}$. Each chip was incubated with a concentration of labelled myoglobin, from 0 to 100 ng/mL. Each concentration was assayed per triplicate. After washing, drying and measuring the fluorescence, the data were treated and plotted against the myoglobin concentration to obtain the sensitivity curve (Figure 4).

The minimum amount of protein that could be distinguished from the blank was 1 ng/mL. The limit of detection (LOD) was defined as the concentration that provides the signal of the blank plus 3 times the standard deviation of the blank. Such concentration was found to be 1 ng/mL.

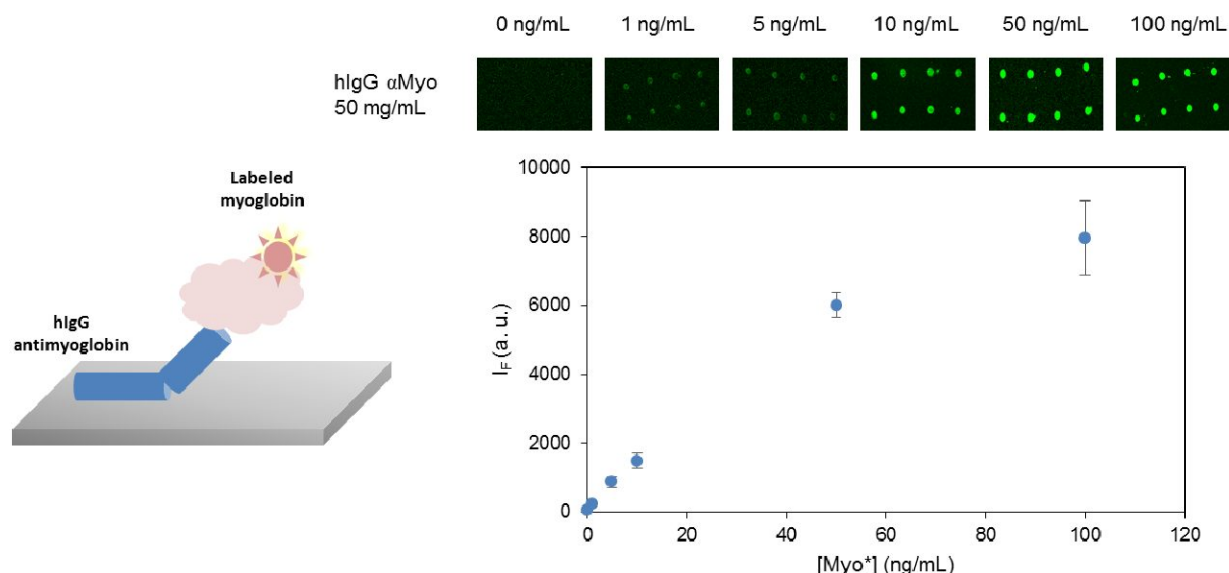


Figure 4. Detection of Myoglobin at different concentrations by direct immunoassay performed on TEC immobilized primary monoclonal anti-Myoglobin antibodies on SOI planar surfaces.

3.2 Monoclonal Anti-Troponin I immobilization with TEC and Immunorecognition

Since cTnI is most unstable to buffer changes it could not be labelled with the Alexa Fluor. Therefore, a sandwich-type immunoassay had to be performed. Thus, the detection of cTnI was done by creating microarrays of the hIgG of monoclonal αcTnI by the TEC methodology as described above, and by incubating such arrays with different cTnI concentrations in 10% diluted human serum, and by finally developing with a labelled detection antibody. This optimised methodology obtained a sensitivity of 10 ng/mL of cTnI (Figure 5) calculated as indicated above for the Myoglobin. The worse sensitivity obtained for the cTnI assay could be due to the type of immunoassay format, including one more step, and that could be in detriment of the final yield. In any case, both for the cTnI and the Myoglobin, the reached sensitivities were within the detection limits of other existing microarray approaches. The good sensitivities were attributed to the proper orientation of the binding sites in the immobilized hIgG, as it was initially expected.

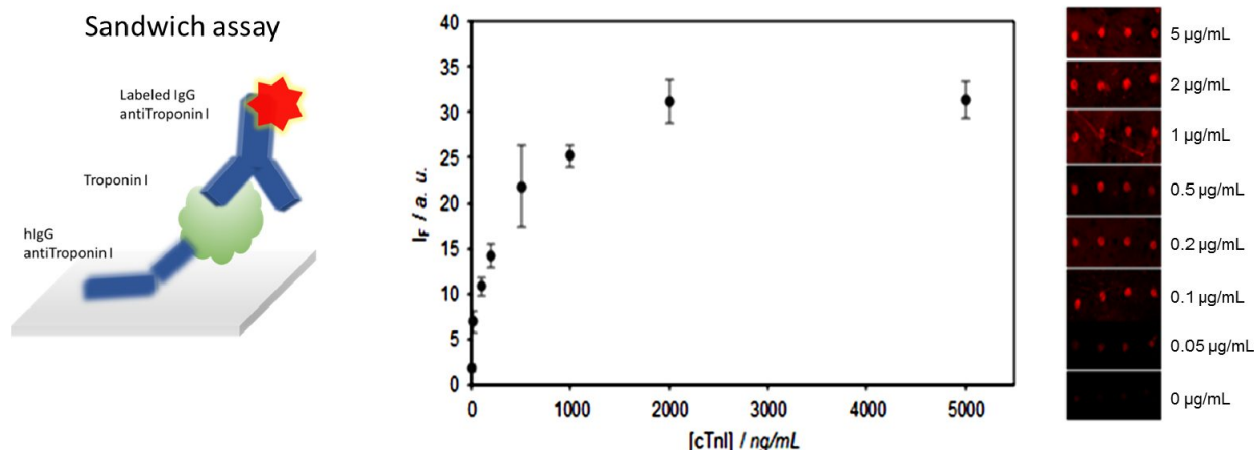


Figure 5. Detection of cTnI at different concentrations by sandwich immunoassay performed on TEC immobilized primary monoclonal anti-cTnI antibodies on SOi planar surfaces.

3.3 Specificity assays

To test the possibility of performing multiplexing assays detecting both proteins at the same time in a sample, microarrays were created containing one row of immobilized hIgG anti-Myoglobin and one row of hIgG anti-cTnI (4 spots/row). The immobilization was performed as explained before (Section 2.2.3).

After that, some of the microarrays were incubated with a sample containing labelled Myoglobin in 10% serum PBS, others with a sample containing cTnI and others with a sample containing an equimolar mixture of both proteins. For those chips incubated with a solution containing cTnI, a further incubation with labelled cTnI antibody was performed. The obtained results are depicted in Figure 6. For hIgG anti-cTnI antibody, no cross reactivity towards the Myoglobin was detected. However, when hIgG anti-Myoglobin antibody was incubated with cTnI and further developed with labelled anti-cTnI antibody, the microarray revealed a residual unspecific recognition. After several control assays it was observed that hIgG anti-Myoglobin antibody recognized unspecifically the detection labelled antibody used in the sandwich cTnI immunoassay. Although the amount of unspecific recognition is low, we believe that this could be totally suppressed by optimizing the conditions for the last incubation step in the sandwich format immunoassay.

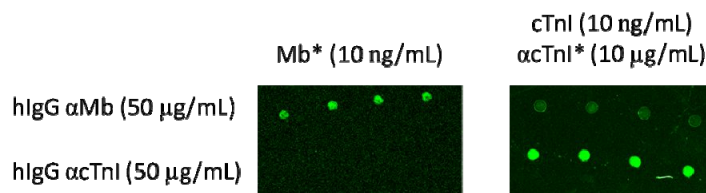


Figure 6. Multiplex assay with TEC immobilization of hIgG anti-Myoglobin and hIgG anti-cTnI to determine specificity and cross reactivity of the immobilized biosensors.

3.4 Monoclonal Anti-Myoglobin immobilization with LAMI and Immunorecognition

The primary anti-Myoglobin antibody was illuminated with 280 nm according to a line pattern (50 lines, 25 μm pitch distance between lines). Direct visualization of the immobilized primary anti-Myoglobin antibody is not possible due to the lack of fluorescent labeling of this biosensor. After immobilization, a sandwich immunoassay was performed using the biomarker Myoglobin and DyLight488 labeled secondary anti-Myoglobin antibody.

In figure 7A (left) is depicted the confocal fluorescence image obtained after performing the sandwich immunoassay.

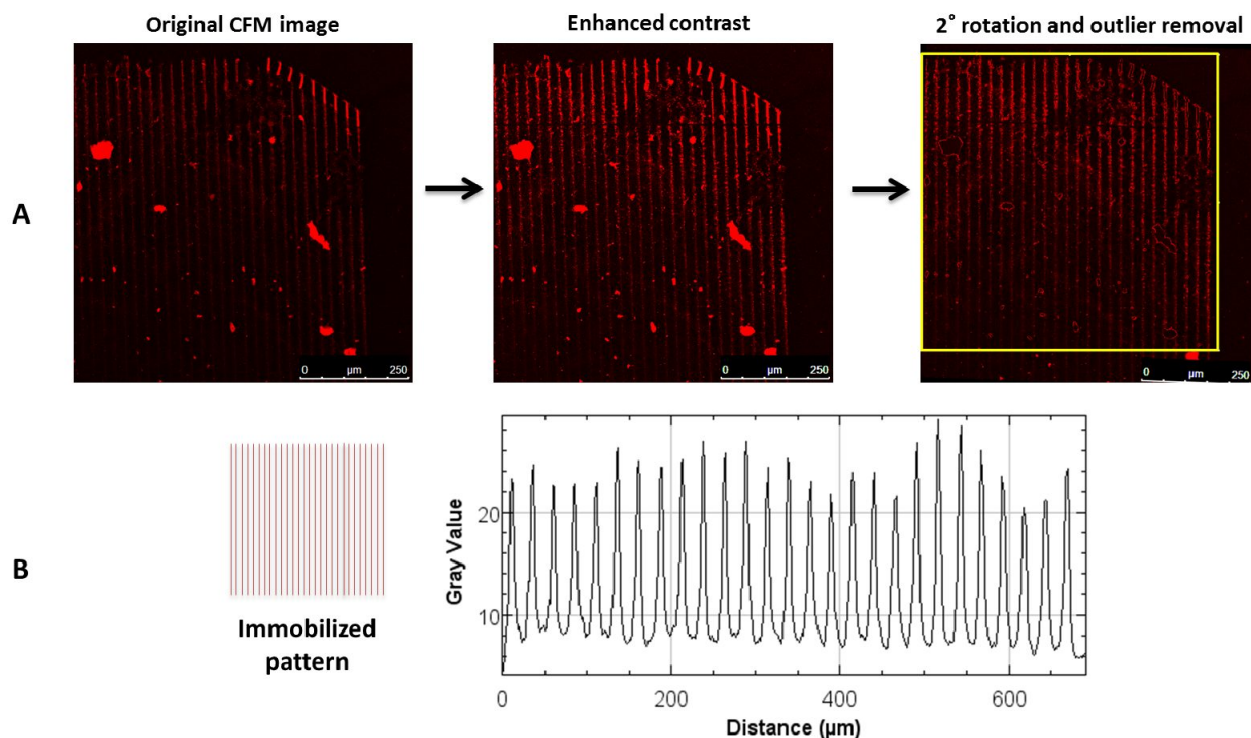


Figure 7. Immobilized biosensor pattern analysis and myoglobin immunodetection. A- *Left*: Confocal fluorescence image of DyLight488 labeled secondary anti-myoglobin antibody after sandwich immunoreaction with 3nM myoglobin and primary monoclonal anti-myoglobin antibody, immobilized according to a lines pattern on SOI thiol derivatized planar surfaces; *Center*: Contrast enhancement of the original CFM image (*left*); *Right*: Outlier removal for pattern analysis. B- Average fluorescence emission intensity profile of the selected area (yellow square) in image A (*right*).

This image depicts the fluorescence intensity detected for the DyLight488 fluorescent secondary anti-Myoglobin antibody. This result shows both that the immobilization of the primary anti-Myoglobin antibody was successful and that the immobilization process (UV illumination) did not hinder the biosensors bioavailability towards the biomarker detection. It is also possible to observe that the immobilized pattern shows a good spatial resolution, although some bright red spots are visible in the original CFM image. To further analyze the pattern's spatial resolution in the original image, image treatment was carried out using the software imageJ. The contrast was enhanced (figure 7A, center) and the image was rotated 2° to the left. An outlier removal was also performed to remove the red spots scattered along the pattern (Figure 7A, right). In the outlier removal command, the software will replace a pixel by the median of the pixels in a given surrounding radius that deviate from the median above a defined threshold. An area was selected on the obtained processed image (yellow box) to obtain an accumulated average fluorescence intensity profile where pixel intensity along the selected area of the image is plotted in function of the distance in μm . The fluorescence intensity profile (figure 7B) shows a periodic and homogenous distribution of the fluorescence intensity peaks (maximum fluorescence emission intensity distribution = 24.5 ± 2.2), where each peak corresponds to a line in the immobilized pattern. The presence of red spots can be attributed to free fluorophore molecules since the labeling kit did not provide a MW separation column. However, the presence of these bright read spots did not interfere with the immunoreaction as, after some image treatment, it is possible to see a homogeneous and resolved fluorescent pattern.

3.5 Monoclonal Anti-Troponin I immobilization with LAMI and Immunorecognition

The primary anti-cTnI antibody was also immobilized onto the planar thiolized SOI surfaces through LAMI. Due to the lack of fluorescent labeling of this biosensor, visualization of the immobilized pattern was possible only after the sandwich immunoassay, as reported also for the primary anti-myoglobin antibodies. In figure 8 A1 and B1 are two CFM images obtained after immunobinding with cTnI and AF647 labeled secondary anti-cTnI antibody. In figure 8A1 is displayed the detection of 4 μ M of cTnI and in image 8B1 is displayed the detection of 4nM of cTnI. In both cases, CFM images show that immobilization and immunorecognition of the biomarker was successful.

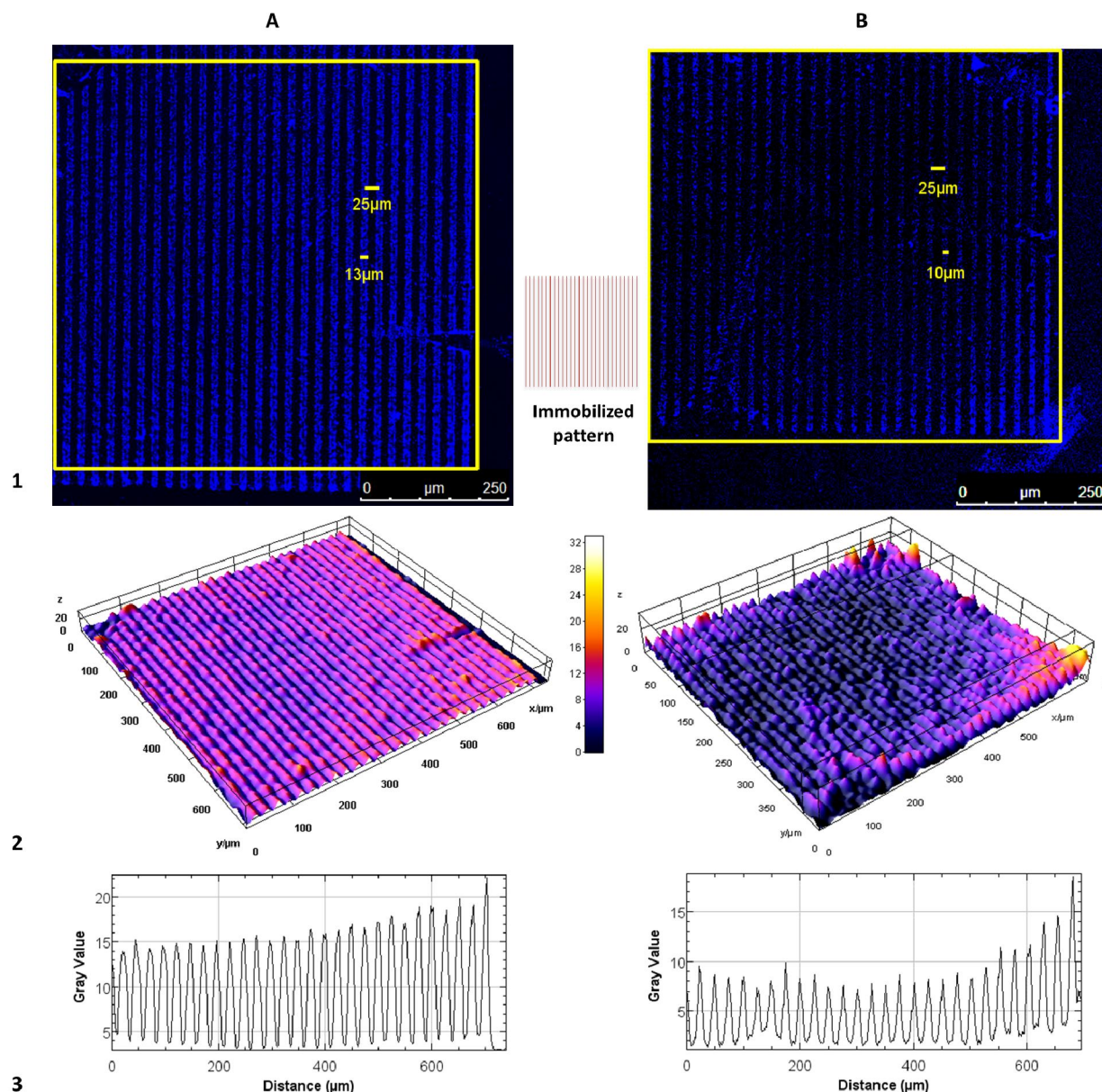


Figure 8. Immobilized biosensor pattern analysis and cTnI immunodetection. A1 and B1- Confocal fluorescence image of AF647 labeled secondary anti-cTnI antibody after sandwich immunoreaction with 4 μ M and 4nM cTnI, respectively, and primary monoclonal anti-cTnI antibody, immobilized according to a lines pattern on SOI thiol derivatized planar surfaces; A2 and B2- 3D surface plot representation of A1 and B1, respectively. A3 and B3- Average fluorescence emission intensity profile of the selected areas (yellow square) in images A1 and B1.

The visualized patterns are very homogenous and resolved. The pitch distance (distance between the center of two consecutive line of the pattern) was 25 μm . This is the distance plotted in the microfabrication stage controlling software, demonstration the precision of the optical setup. The line width obtained in each pattern was also measured. In figure A1 the line width obtained was 13 μm while in figure B1 was 10 μm . This might be explained by the different concentrations of cTnI detected by the pattern immobilized biosensors. Higher concentration of cTnI resulted in a 3 μm detection pattern.

Further analysis was performed on the images. In figures 8A2 and 8B2 are depicted 3D surface plots obtained from the analysis of a selected area (yellow squares) of figures 8A1 and 8B1, respectively. In this analysis, the fluorescence intensity values are translated as the height of the plot, translated into a colorimetric scale. The pattern where a higher concentration of cTnI was detected (Figure 8A2) shows a very homogeneous intensity distribution as the plot for the lines pattern is fairly monochromatic. The 3D surface plot obtained for the immobilized pattern which detected a lower concentration of cTnI (Figure 8B2) displays a less homogeneous intensity distribution, particularly in the lower right corner of the pattern. The results visualized in both 3D surface plots are confirmed by the average fluorescence emission intensity profile obtained for the selected areas (yellow squares) in images A1 and B1 (Figure 8 A3 and B3, respectively). The intensity profiles show peaks with homogeneous width, each peak representing an individual line of the pattern. The differences in fluorescence intensity can be explained by the biosensor distribution on the SOI surface upon immobilization. When placing the droplets for immobilization, these droplets display a slightly higher concentration of biosensor on the edges of the droplet in a “donut effect” that results from the surface hydrophobicity (as a result of the thiol chemistry applied to the surfaces for LAMI immobilization). Thus, the pattern area immobilized in these edges will display higher fluorescence intensity.

4. CONCLUSION

The immobilization of both biosensors, primary monoclonal anti-myoglobin and anti-cTnI antibodies, was successfully achieved by TEC and LAMI. Furthermore, the bioavailability of both biosensors was not compromised by the photonic immobilization techniques used, as demonstrated through immunoassays. Thus, both techniques are suitable for biosensor immobilization for POCT devices and are currently being applied in the development of a POCT device for early detection of cardiovascular diseases.

5. ACKNOWLEDGMENTS

The authors acknowledge the funding from the European Commission through the projects H2020-634013-2-PHOCNOSIS and H2020-644242 –SAPHELY.

6. REFERENCES

- [1] “WHO Cardiovascular diseases (CVDs).”, WHO, 2017, <<http://www.who.int/mediacentre/factsheets/fs317/en/>> (28 February 2018).
- [2] Vasan, R. S., “Biomarkers of cardiovascular disease: Molecular basis and practical considerations,” *Circulation* **113**(19), 2335–2362 (2006).
- [3] Dhingra, R., Vasan, R. S., “Biomarkers in cardiovascular disease: Statistical assessment and section on key novel heart failure biomarkers,” *Trends Cardiovasc. Med.* **27**(2), 123–133 (2017).
- [4] Qureshi, A., Gurbuz, Y., Niazi, J. H., “Sensors and Actuators B : Chemical Biosensors for cardiac biomarkers detection : A review,” *Sensors Actuators B. Chem.* **171–172**, 62–76 (2012).
- [5] Babuin, L., Jaffe, A. S., “Troponin: The biomarker of choice for the detection of cardiac injury,” *Cmaj* **173**(10), 1191–1202 (2005).
- [6] Solaro, R.J, Rosevear,P., Kobayashi,T., “The unique functions of cardiac troponin I in the control of cardiac muscle contraction and relaxation,” *Biochem Biophys Res Commun* **369**(1), 82–87 (2009).

- [7] Takeda, S., Yamashita, A., Maeda, K., Maéda, Y., "Structure of the core domain of human cardiac troponin in the Ca^{2+} -saturated form," *Nature* **424**, 35–42 (2003).
- [8] Schreier, T., Kedes, L., Gahlmann, R., "Cloning, Structural Analysis, and Expression of the Human Slow Twitch Skeletal Muscle / Cardiac Troponin C Gene *," *J Biol Chem* **265**(34), 21247–21253 (1990).
- [9] Slot, M. H. E. B., Heijden, G. J. M. G., Stelpstra, S. D., Hoes, A. W., Rutten, F. H., "Point-of-care tests in suspected acute myocardial infarction: A systematic review," *Int. J. Cardiol.* **168**(6), 5355–5362 (2013).
- [10] Friess, U., Stark, M., "Cardiac markers: a clear cause for point-of-care testing," *Anal Bioanal Chem* **393**, 1453–1462 (2009).
- [11] Luka, G., Ahmadi, A., Najjaran, H., Alocilja, E., DeRosa, M., Wolthers, K., Malki, A., Aziz, H., Althani, A., Hoorfar, M., "Microfluidics Integrated Biosensors: A Leading Technology towards Lab-on-a-Chip and Sensing Applications," *Sensors* **15**, 30011–30031 (2015).
- [12] Kolb, H. C., Finn, M. G., Sharpless, K. B., "Click Chemistry: Diverse Chemical Function from a Few Good Reactions," *Angew. Chem. Int. Ed.* **40**, 2004–2021 (2001).
- [13] Dondoni, A., "The Emergence of Thiol – Ene Coupling as a Click Process for Materials and Bioorganic Chemistry," *Angew. Chem. Int. Ed.* **47**, 8995–8997 (2008).
- [14] Hoyle, C. E., Bowman, C. N., "Polymer Chemistry Thiol – Ene Click Chemistry," *Angew. Chem. Int. Ed.* **49**, 1540–1573 (2010).
- [15] Escorihuela, J., Bañuls, M. J., Puchades, R., Maquieira, Á., "Development of Oligonucleotide Microarrays onto Si-Based Surfaces via Thioether Linkage Mediated by UV Irradiation" *Bioconjugate Chem.* **23**, 2121–2128 (2012).
- [16] Escorihuela, J., Bañuls, M. J., Puchades, R., Maquieira, Á., "DNA microarrays on silicon surfaces through thiol-ene chemistry," *Chem. Commun.* **48**, 2116–2118 (2012).
- [17] Escorihuela, J., Bañuls, M. J., Grijalvo, S., Eritja, R., Puchades, R., Maquieira, Á., "Direct Covalent Attachment of DNA Microarrays by Rapid Thiol – Ene 'Click' Chemistry," *Bioconjugate Chem.* **25**(3), 618–627 (2014).
- [18] Neves-Petersen, M. T., Gryczynski, Z., Lakowicz, J., Fojan, P., Pedersen, S., Petersen, E., Petersen, S. B., "High probability of disrupting a disulphide bridge mediated by an endogenous excited tryptophan residue," *Protein Sci.* **11**(3), 588–600 (2002).
- [19] Neves-Petersen, M. T., Snabe, T., Klitgaard, S., Duroux, M., Petersen, S. B., "Photonic activation of disulfide bridges achieves oriented protein immobilization on biosensor surfaces," *Protein Sci.* **15**(2), 343–351 (2006).
- [20] Ioerger, T. R., Du, C., Linthicum, D. S., "Conservation of cys-cys trp structural triads and their geometry in the protein domains of immunoglobulin superfamily members," *Mol. Immunol.* **36**(6), 373–386 (1999).
- [21] Parracino, A., Neves-Petersen, M. T., di Gennaro, A. K., Pettersson, K., Lövgren, T., Petersen, S. B., "Arraying prostate specific antigen PSA and Fab anti-PSA using light-assisted molecular immobilization technology," *Protein Sci.* **19**(9), 1751–1759 (2010).
- [22] Skovsen, E., Kold, A. B., Neves-Petersen, M. T., Petersen, S. B., "Photonic immobilization of high-density protein arrays using Fourier optics," *Proteomics* **9**(15), 3945–3948 (2009).
- [23] Parracino, A., Gajula, G. P., di Gennaro, A. K., Correia, M., Neves-Petersen, M. T., Rafaelsen, J.,

- Petersen, S. B., "Photonic immobilization of BSA for nanobiomedical applications: Creation of high density microarrays and superparamagnetic bioconjugates," *Biotechnol. Bioeng.* **108**(5), 999–1010 (2011).
- [24] Petersen, S. B., di Gennaro, A. K., Neves-Petersen, M. T., Skovsen, E., Parracino, A., "Immobilization of biomolecules onto surfaces according to ultraviolet light diffraction patterns.," *Appl. Opt.* **49**(28), 5344–5350 (2010).
- [25] Duroux, M., Skovsen, E., Neves-Petersen, M. T., Duroux, L., Gurevich, L., Petersen, S. B., "Light-induced immobilisation of biomolecules as an attractive alternative to microdroplet dispensing-based arraying technologies," *Proteomics* **7**(19), 3491–3499 (2007).
- [26] Bent, D. V., Hayon, E., "Excited state chemistry of aromatic amino acids and related peptides. II. Phenylalanine," *J. Am. Chem. Soc.* **97**(10), 2606–2612 (1975).
- [27] Bent, D. V., Hayon, E., "Excited state chemistry of aromatic amino acids and related peptides. III. Tryptophan," *J. Am. Chem. Soc.* **97**(10), 2612–2619 (1975).
- [28] Bent, D. V., Hayon, E., "Excited state chemistry of aromatic amino acids and related peptides. I. Tyrosine," *J. Am. Chem. Soc.* **97**(10), 2599–2606 (1975).
- [29] Neves-Petersen, M. T., Klitgaard, S., Pascher, T., Skovsen, E., Polivka, T., Yartsev, A., Sundström, V., Petersen, S. B., "Flash photolysis of cutinase: Identification and decay kinetics of transient intermediates formed upon UV excitation of aromatic residues," *Biophys. J.* **97**(1), 211–226 (2009).
- [30] Correia, M., Neves-Petersen, M. T., Jeppesen, P. B., Gregersen, S., Petersen, S. B., "UV-light exposure of insulin: pharmaceutical implications upon covalent insulin dityrosine dimerization and disulphide bond photolysis.," *PLoS One* **7**(12), e50733 (2012).
- [31] Correia, M., Snabe, T., Thiagarajan, V., Petersen, S. B., Campos, S. R. R., Baptista, A. M., Neves-Petersen, M. T., "Photonic Activation of Plasminogen Induced by Low Dose UVB," *PLoS One* **10**(1), e0116737 (2015).
- [32] Gonçalves, O., Snider, S., Zadoyan, R., Nguyen, Q.-T., Vorum, H., Petersen, S. B., Neves-Petersen, M. T., "Novel microfabrication stage allowing for one-photon and multi-photon Light Assisted Molecular Immobilization and for multi-photon microscope," *Proc.SPIE* 10079, 100790F (2017) (2017).
- [33] Correia, M., Neves-Petersen, M. T., Parracino, A., di Gennaro, A. K., Petersen, S. B., "Photophysics, photochemistry and energetics of UV light induced disulphide bridge disruption in apo- α -lactalbumin," *J. Fluoresc.* **22**(1), 323–337 (2012).
- [34] Silva, C. O., Petersen, S. B., Pinto Reis, C., Rijo, P., Molpeceres, J., Vorum, H., Neves-Petersen, M. T., "Lysozyme photochemistry as a function of temperature. the protective effect of nanoparticles on lysozyme photostability," *PLoS One* **10**(12), 1–29 (2015).